Comparison of Probe Materials for Tissue Cryoablation: Operational Properties of Metal and Sapphire Cryoprobes

Aleksandr V. Pushkarev[1*], Sergey S. Ryabikin[1], Dmitry I. Tsiganov[1], Arsen K. Zotov[1,2], Vladimir N. Kurlov[1,2], and Irina N. Dolganova[1,2]**

[1] Bauman Moscow State Technical University, 5 Baumanskaya 2nd str., Moscow 105005, Russia

[2] Osipyan Institute of Solid State Physics of the Russian Academy of Sciences, 2 Academician Osipyan str., Moscow District, Chernogolovka 142432, Russia

*** e-mail:** pushkarev@bmstu.ru

**** e-mail:** dolganova@issp.ac.ru

Abstract. Typical probes that are used for cryosurgical applications are manufactured from metals, since such materials as copper and brass feature high thermal conductivity at low temperatures and enable rapid growth of an ice ball in living tissues. Due to a favorable combination of properties, sapphire could be also widely used for tissue cryoablation. In this paper, a sapphire probe is experimentally compared with metal ones. Using a gel-based biotissue phantom, an ice ball volume and phantom temperatures in control points are analyzed for the considered probe materials aimed at revealing the advantages of using sapphire for cryosurgery. Next, the impact of probe-tissue contact on the sample and probe surface is studied. The experimental results and qualitative comparison of the considered cryoprobes demonstrate the abilities of the sapphire one for faster tissue freezing, reaching lower temperatures and featuring less damage of its contact surface and adjacent tissues, justifying a potential of sapphire as a material for tissue cryosurgery. © 2022 Journal of Biomedical Photonics & Engineering.

Keywords: cryosurgery; tissue ablation; ice ball; cryoprobe; sapphire probe.

Paper #3505 received 30 Jun 2022; revised manuscript received 15 Oct 2022; accepted for publication 16 Oct 2022; published online 23 Nov 2022. doi: 10.18287/JBPE22.08.040501.

1 Introduction

Cryoablation is the procedure of tissue damaging by their freezing [1, 2]. The main mechanisms of the cell death underlying the cryoablation are the appearance of intracellular and extracellular ice crystals in tissue, osmotic injury, hypoxia, and cell apoptosis [3, 4]. Cryoablation as a method of medical treatment is often used for abnormal tissues, in particular, malignant, and is considered as an alternative approach to conventional surgical resection in some cases, since it is relatively minimally invasive, well-tolerated and less painful.

For the first time, tissue freezing was performed more than 150 years ago by James Arnott [5]. And since the introduction of the first system for cryosurgery [6], the instrumentation and technique for tissue cryoablation were improved significantly. The development of technology and navigation methods resulted in the fact that cryosurgical approaches today are applied in oncology, dermatology, urology and other fields for treatment of such diseases as renal [7, 8], hepatic [9], endometrial [4], lung [10], prostate [11], breast cancer [12–14], skin melanoma [15], as well as chronic rhinitis [16], and oral lesion [17].

Despite the variety of nosologies and localizations of tissue lesions that can be treated by cryoablation, it is possible to distinguish percutaneous and superficial applications. Percutaneous cryoablation implies thin needle-like probes, which are often based on Joule-Thomson effect and flow of high-pressure gas, for example, argon [12, 18–22]. Such probes can be even combined with an endoscope, since it is possible to make them flexible and thermally insulated, except for metal tips that are in the direct contact with tissues [23]. However, Ar-based cryoprobes require special safety procedures. In contrast, for superficial cryoablation, probes of different size and shape are applied. In addition

to Joule-Thomson effect, these probes of submersible and flowing types can be cooled down by the contact with circulating or stored coolant, for instance, liquid nitrogen [14, 24–26], which is less complicated than operation with high-pressure gas.

Both superficial and percutaneous cryoprobes should meet a number of requirements:

– biocompatibility and chemical inertness of the tip;
– provide the tissue cooling rate that ensures the ablation;
– enable rapid cooling down;
– admit one or several techniques of monitoring of the freezing process to prevent damaging of the adjacent healthy tissues and complete freezing of the tissue lesion.

According to them, commercially available probes and/or their tips are made of various metals, most commonly of stainless steel, aluminum, copper, or brass [27–29]. These materials ensure ablation of tissues and allow manufacturing of complex shape and various dimensions of the probes. However, such probes and tips are often disposable, since they do not withstand strong sterilization methods. Despite conventional imaging techniques for control of the tissue ice ball formation, such as ultrasound imaging (US) and computed tomography (CT), can be realized with these instruments, only a few types of probes can be combined with magnetic resonance imaging (MRI).

Besides metal materials, sapphire also meets the requirements for efficient cryoablation [30]. It combines high thermal conductivity at low temperature, chemical inertness and resistance, biocompatibility and high hardness [31]. The latter makes it difficult to manufacture sapphire cryoprobes with complex shape. However, application of the Stepanov concept for crystal growth, in particular, the edge-defined film-fed growth (EFG) and non-capillary shaping (NCS) techniques [32–35], makes it possible to obtain sapphire crystals of various form, size, shape, and reduces the need of mechanical processing to the minimal level. Such growth methods equipped with the automated system of crystal weight control [36] provide maintaining of the desired form and ensure high quality of the growing crystal. The mentioned properties and growth techniques pave the way for considering sapphire as a material for tissue cryoablation.

In this paper, we qualitatively compare the capabilities of typical metal cryoprobes with the sapphire one grown by the EFG technique, making them of the same size and shape. The manufactured copper, brass, and sapphire probes of the submersible type were equally cooled down by the same method using liquid nitrogen as the coolant. We analyzed the dynamics and dimensions of the ice ball formation in the ultrasonic gel phantom, measuring the temperature of the probe surface, as well as at two depths inside the phantom, and visualizing the ice ball shape using digital camera. Then we qualitatively compared the condition of the probe surfaces after a routine application and the effect of tissue sticking to the probe using *ex vivo* tissue samples.

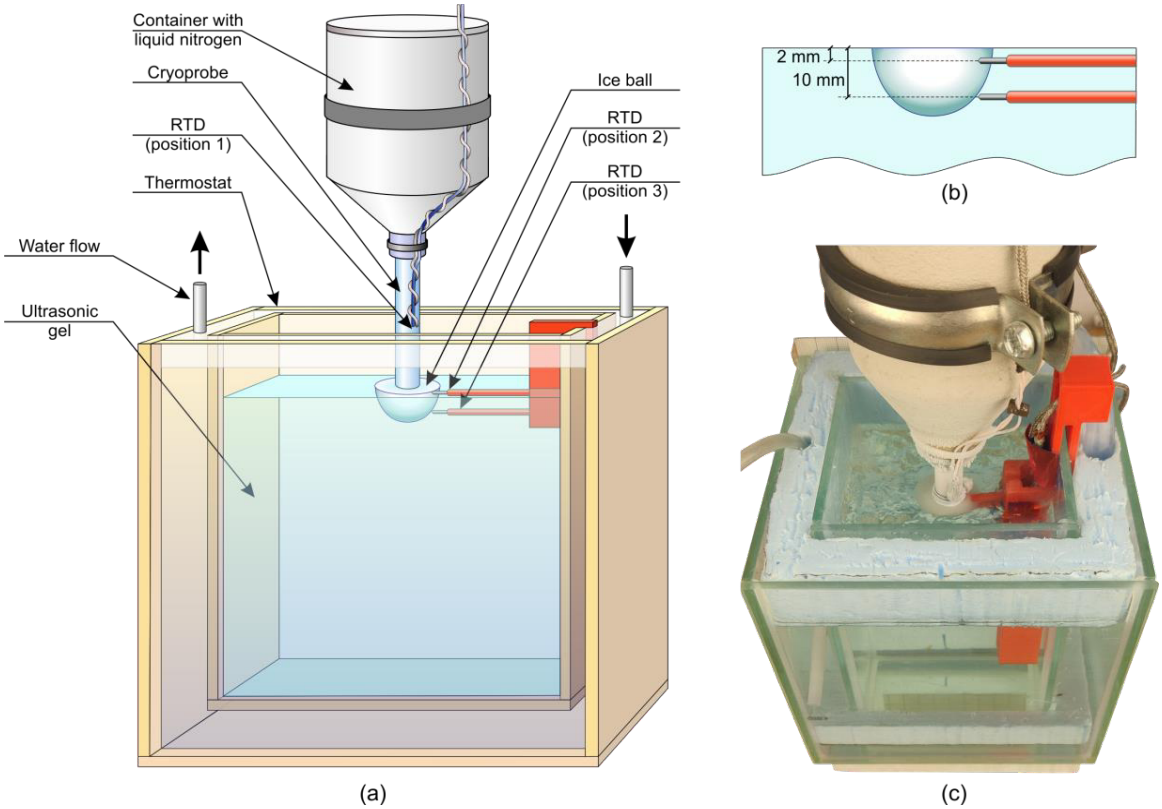

Fig. 1 Measurement of the ice ball formation. (a) Schematic of the experimental setup, where RTD stands for a resistance temperature detector. (b) Positions of the RTDs fixed inside the ultrasonic gel volume. (c) Photo of the experimental setup.

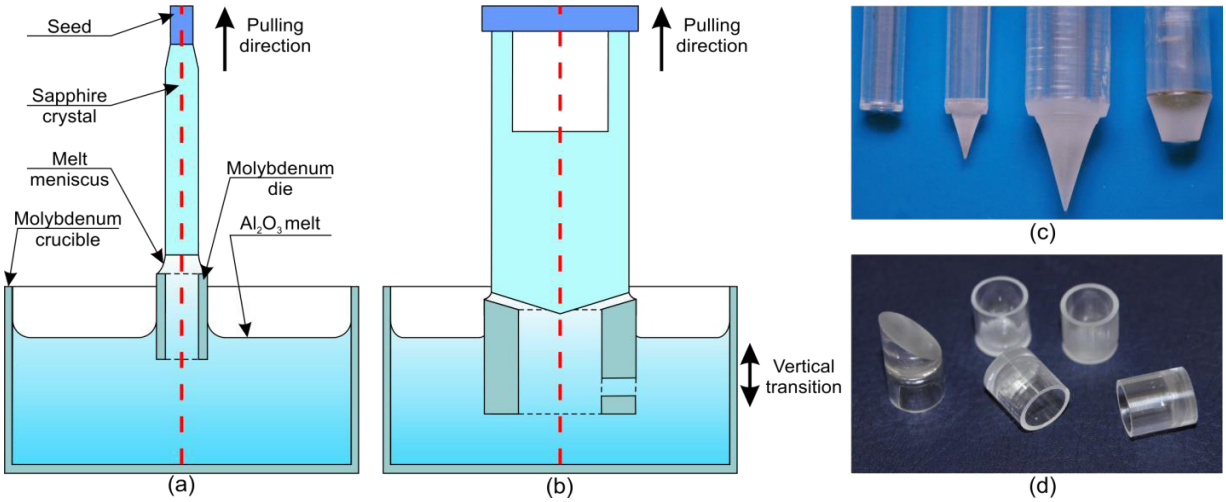

Fig. 2 Schematic of the sapphire shaped crystal growth (a) by the EFG technique, (b) by the NCS technique. (c), (d) Representative examples of sapphire cryoprobes of different shape.

According to the obtained results, the sapphire probe ensures faster cooling down to the desired temperature. Thus, produced ice ball possesses larger volume, while the freezing dynamics is also higher for the sapphire than for the metal probes, completely satisfying the required freezing rate. Due to lower temperature of the sapphire probe contact surface, no tissue-sticking effect was noticed. Finally, the microscopic images of the sapphire probe show less damage after application, in contrast to the metal ones highlighting the advantage of being reusable.

The experimental results confirm the possibility of using sapphire for cryosurgery and treatment, since its capabilities for cryoablation surpass those of metal. Although we consider submersible types of metal and sapphire probes, the same properties are expected for other types. Application of EFG and NCS growth techniques allows for making such probes of desirable shape and size. The results of this study pave the way of implementing sapphire for modern cryosurgical procedures.

2 Materials and Methods

2.1 Ice Ball Formation Using Gel-Based Biotissue Phantoms

The capabilities of the metal and sapphire cryoprobes to form ice balls were studied during an experiment. For the visualization of the ice balls, the “Mediagel” ultrasonic gel (manufactured by Geltek-Medica, Moscow, Russia) was used as a biotissue phantom. It had thermal properties similar to biotissues [37, 38]. The 90×90×90 mm gel-based biotissue phantom was heated to 37 °C. It was placed in the water-based thermostat (Termex, Tomsk, Russia, ±0.1 °C) to maintain the stable temperature near the borders (see schematic and a photo in Fig. 1). The ambient temperature was 24 °C.

The cryoprobe was cooled and then touched the phantom surface. The process of the ice ball formation was recorded by a camera in order to estimate the ice ball dimensions. The measurement errors were no more than 1 mm. The temperature measurements were performed by the three resistance temperature detectors (class A, Heraeus Sensor Technology, Hanau, Germany). The temperature detectors were calibrated using a set of the measuring equipment of the third category: a platinum resistance reference thermometer (PTSV-2/3/65, ELEMER, Ltd., Zelenograd, Russia) and a digital reference thermometer (TCE 005, ELEMER, Ltd., Zelenograd, Russia) in accordance with the State Verification Scheme (GOST 8.558-2009). For this aim, the method of direct comparison was used. The measurement errors were no more than 0.5 °C at temperatures below the end of the freezing of the biotissue phantom. The positions of RTD are shown in Figs. 1 (a) and (b). The first detector measured the probe surface temperature, the second and third ones were fixed inside the phantom at depths 2 and 10 mm.

2.2 Sapphire Probe Manufacturing

The sapphire cryoprobes are manufactured by the EFG technique of crystal growth from Al_2O_3 melt [32–34] (Fig. 2 (a)). It implies the growth chamber, the high purity Ar atmosphere as an ambient, which is under the pressure of 1.1–1.3 atm, the 22 kHz induction-heated graphite susceptor/molibdenium crucible setup, the die with one or several capillary channels that determines the shape of the grown crystal, and the crushed Verneuil crystal as a feed material. The melt rises up through the capillary channels and forms the meniscus on the top of the wettable die. The pulling rate of thus produced crystal is within the ranges from 4 to 6 cm/h. The high quality of the grown crystals and the almost absence of defects is provided by the relatively low pulling rate and the applied weight control system based on a precise weight sensor. In addition, NCS technique can be used instead of EFG for manufacturing of sapphire rods and tubes of large diameters [35] (Fig. 2 (b)). NCS implies melt

delivering to the growth surface through the non-capillary channel. It is also suitable for segmented rods with transition from bulk crystal to hollow one [35, 39]. A variety of shapes and geometries of cryoprobes that can be achieved by the crystal growth techniques is rather wide. Representative examples of sapphire probes and tips are demonstrated in Figs. 2 (c) and (d).

The complex form of the die along with maintaining of the technological parameters of the growth process enable the appearance of internal either closed or open channels in a crystal with significant variation of diameters, from several hundreds of microns up to several centimeters [35, 39, 40–43]. For this aim, no additional mechanical processing is needed. The altering of the crystal shape along its length, particularly, the transition from the bulk shape to the tube-like one (Fig. 2(b)), could be potentially used for storing coolant, maintaining more effectively the temperature of the sapphire cryoprobe and reducing the overall dimensions of the cryosurgical equipment.

3 Results and Discussion

Several physical properties that determine the performance of copper, brass and sapphire cryoprobes are compared in Table 1 [31, 44, 45]. Higher thermal conductivity and lower specific heat at cryogenic temperatures (77 K) of sapphire in comparison to metals imply the possibility to achieve high cooling rate of the material itself as well as an ambient and to maintain low temperature of a tissue that results in tissue cryonecrosis [46–49]. High melting point, hardness and solubility in acids open a wide range of methods for probe cleaning and sterilization. Thus, the sapphire seems to be a prospective material for making reusable cryoprobes.

Table 1 Physical properties of cryoprobe materials.

	Melting point, °C	Thermal conductivity at 77 K, W/(m·K)	Thermal conductivity at 300 K, W/(m·K)	Specific heat capacity at 77 K, 10^{-3} J/(kg·K)	Specific heat capacity at 300 K, 10^{-3} J/(kg·K)	Hardness, Mohs	Solubility in HNO_3, H_2SO_4, HCl, HF
Copper	1085	544	397	0.192	0.386	3	–
Brass	900–940	29	86	0.216	0.377	3	–
Sapphire	2050	1100	47	0.060	0.779	9	Insoluble up to 300 °C

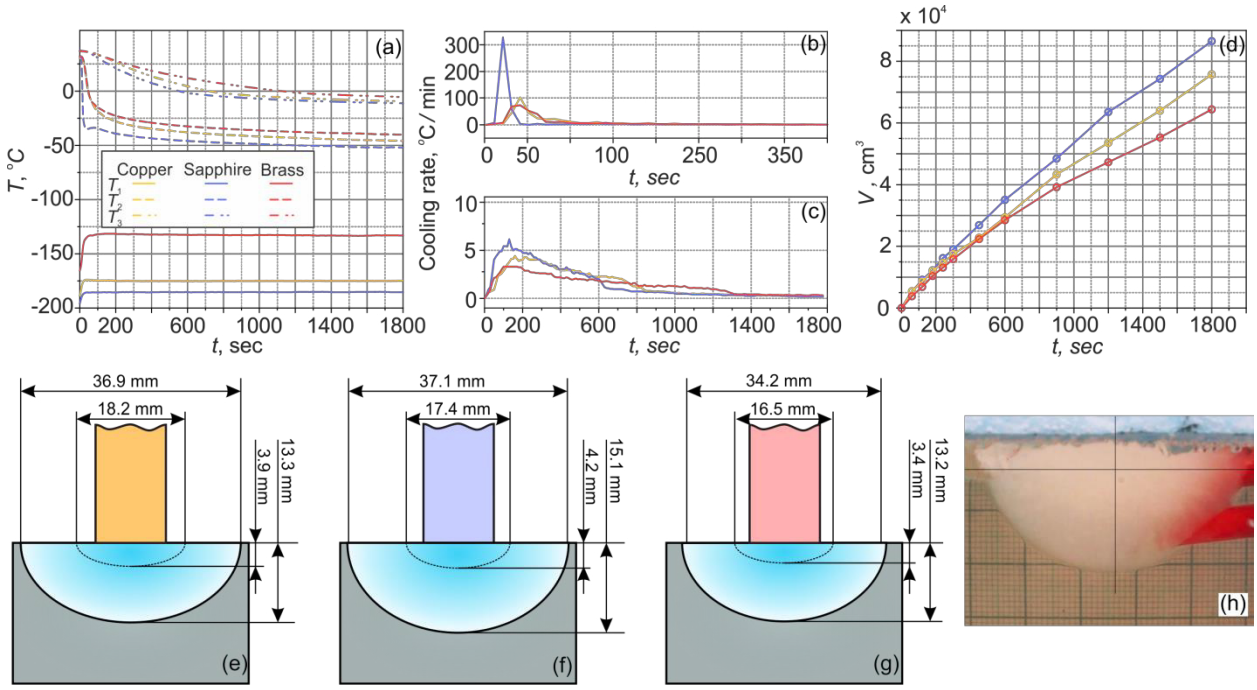

Fig. 3 The performance of copper, brass and sapphire cryoprobes studied by means of gel-based biotissue phantom. (a) Temperature dynamics measured at the probe surface (T_1), at depth of 2 mm (T_2) and 10 mm (T_3) in the sample volume. Cooling rates at the depths of 2 mm (b) and 10 mm (c). (d) Ice ball volume obtained by the considered probes. Ice ball geometry estimated after 60 and 1800 sec since the sample contact with the copper (e), sapphire (f), and brass (g) probes. (h) A representing example of the ice ball grown in the ultrasonic gel-based biotissue phantom.

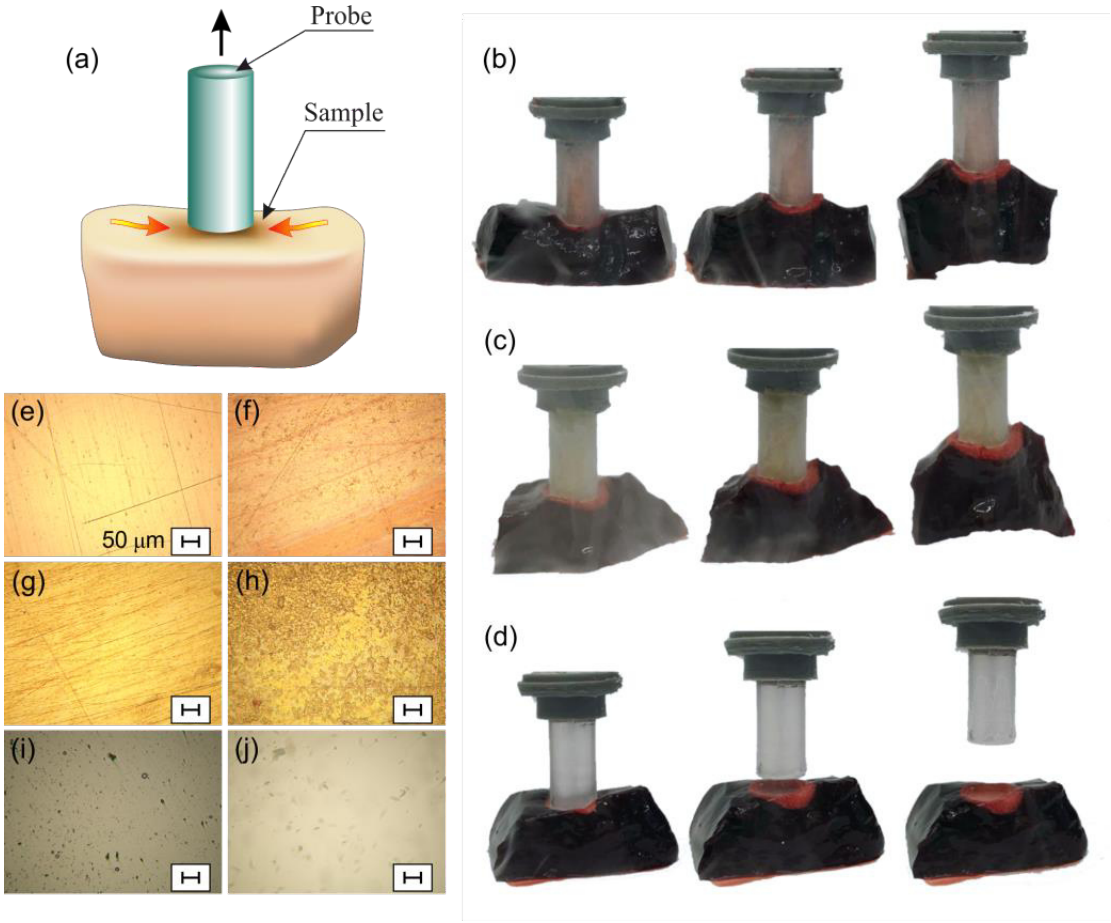

Fig. 4 The impact of the probe-tissue contact. (a) Schematic of the probe lifted after the contact with tissue. Observation of the tissue adherence to the copper (b), brass (c), and sapphire (d) probes. Microscopic images of (e), (f) the copper, (g), (h) the brass, and (i), (j) the sapphire probe surfaces before (left column) and after (right column) *ex vivo* application.

To compare the performance of the considered probes, they were tested experimentally, as described above in Section 2. The copper, brass and sapphire probes with a diameter of 11 mm and a length of 18 cm had a mass of 152 g, 143 g and 68.5 g, respectively. The probes were cooled down and used for a formation of ice balls in a gel-based biotissue phantom, while the temperature was measured in three different points by means of resistance temperature detectors (RTD). The same geometry and the same pressure of each probe on the phantom make it possible to compare the freezing process itself without taking into account the influence of the shape of the instrument. The measured temperature dynamics is shown in Fig. 3(a). It stems from the results that sapphire features lower temperature of its surface near the value of liquid nitrogen. It leads to lower temperatures and faster freezing in the sample volume at the depths of 2 and 10 mm from the surface (see panels (a), (b), and (c) in Fig. 3). As it is followed from the ability to achieve lower temperatures, the sapphire probe produces ice balls of larger volume (panels from (d) to (g) in Fig. 3). This parameter implies the potential volume of tissue cryonecrosis that can be produced via single application.

After comparing the freezing process performed by the considered cryoprobes, we studied the impact of a single cryoapplication on the probe contact surface. For this aim, a short 15-sec contact of preliminary polished probes with the *ex vivo* bovine liver specimen was performed (Fig. 4 (a)). It is seen form panels in Fig. 4 (e–j) that initially the sapphire probe features higher surface quality comparing to the metal ones. Moreover, the degradation of surface and appearance of tissue adherent scarp are obvious for copper and brass, while the sapphire probe almost retains its surface condition and remains untouched.

The appearance of tissue adherent particles on the copper and brass probes are confirmed by the presence of tissue sticking effect after the application (Fig. 4 (b–d)). The images show the probe raising to heights of 4 mm and 8 mm and detachment. The noticeable sticking of the sample to the metal probes is observed, while the sapphire probe effortlessly disconnects from the sample. It highlights that the sapphire probe does not cause additional tension in the adjacent tissues, which can be a source of unpredictable tissue damages.

According to the obtained results, sapphire is a prospective material for cryoprobes manufacturing. It is worth mentioning that crystal growth techniques give

opportunities for making sapphire crystals of various geometry covering wide range of diameters and lengths. Moreover, EFG technique allows for manufacturing of crystals with complex cross-section, having internal channels, which can serve either for coolant circulation or light delivering to tissues when accommodating optical fibers inside these channels. In the latter case, thanks to high transparency of sapphire in visible and near-infrared ranges, if the fiber is connected to the light source, the cryoprobe could perform additional laser ablation or provide diagnostic functions. Finally, sapphire is non-magnetic material, thus, its application can be accompanied by MRI monitoring of cryosurgical process.

4 Conclusions

In this paper, we qualitatively compare the performance of metal and sapphire cryoprobes. The temperature measurements, estimation of the sample cooling rate and ice ball volume reveal the advantages of sapphire over copper and brass. The higher cooling rate and larger ice balls obtained by the sapphire probe confirm the ability of achieving tissue cryonecrosis in larger volume during a single application. In addition, almost absence of tissue adhesion to the sapphire probe and its ability to retain its contact surface undamaged along with high thermal and chemical stability highlight the ability of sapphire cryoprobes for being reusable. Our results demonstrate high potential of sapphire cryoprobes for medical application.

Disclosures

The authors declare no conflict of interest.

Acknowledgments

The authors would like to thank the Bauman Moscow State Technical University for copper and brass probes manufacturing, Osipyan Institute of Solid State Physics of the Russian Academy of Sciences for sapphire probe manufacturing. Biotissue phantom freezing experiments, analysis the dynamics and dimensions of the ice ball formation and temperature data were supported by the Russian Science Foundation (Project #21-19-00676). Experimental estimation of the probe surface conditions after a routine application and the effect of tissue sticking to the probe using *ex vivo* tissue samples were supported by the Russian Science Foundation (Project #19-79-10212-P).

References

1. J. G. Baust, A. A. Gage, "The molecular basis of cryosurgery," BJU International 95(9), 1187–1191 (2005).
2. A. Gage, J. Baust, and J. Baust, "Experimental cryosurgery investigations in vivo," Cryobiology 59, 229–243 (2009).
3. J. P. Erinjeri, T. W. Clark, "Cryoablation: Mechanism of action and devices," Journal of Vascular and Interventional Radiology 21(8), S187–S191 (2010).
4. X. Yang, C. Wang, X. Sun, Q. Fan, J. Yuan, Y. Li, and Y. Wang, "Cryoablation used in fertility-sparing treatment for early endometrial cancer: A pig model experiment using a new designed balloon cryoprobe," Cryobiology 94, 89–94 (2020).
5. J. Arnott, On the Treatment of Cancer: by the Regulated Application of an Anaesthetic Temperature, Churchill, London, England (1851).
6. I. S. Cooper, S. Stellar, "Cryogenic freezing of brain tumors for excision or destruction in situ," Journal of Neurosurgery 20(11), 921–930 (1963).
7. D. A. Kunkle, R. G. Uzzo, "Cryoablation or radiofrequency ablation of the small renal mass," Cancer 113(10), 2671–2680 (2008).
8. W. Deng, L. Chen, Y. Wang, X. Liu, G. Wang, W. Liu, C. Zhang, X. Zhou, Y. Li, and B. Fu, "Cryoablation versus partial nephrectomy for clinical stage T1 renal masses: A systematic review and meta-analysis," Journal of Cancer 10(5), 1226–1236 (2019).
9. C. Wang, H. Wang, W. Yang, K. Hu, H. Xie, K.-Q. Hu, W. Bai, Z. Dong, Y. Lu, Z. Zeng, M. Lou, H. Wang, X. Gao, X. Chang, L. An, J. Qu, J. Li, and Y. Yang, "Multicenter randomized controlled trial of percutaneous cryoablation versus radiofrequency ablation in hepatocellular carcinoma," Hepatology 61(5), 1579–1590 (2015).
10. H. Yashiro, S. Nakatsuka, M. Inoue, M. Kawamura, N. Tsukada, K. Asakura, Y. Yamauchi, K. Hashimoto, and S. Kuribayashi, "Factors affecting local progression after percutaneous cryoablation of lung tumors," Journal of Vascular and Interventional Radiology 24(6), 813–821 (2013).
11. W. P. Tan, A. Chang, C. Sze, and T. J. Polascik, "Oncological and functional outcomes of patients undergoing individualized partial gland cryoablation of the prostate: A single-institution experience," Journal of Endourology 35(9), 1290–1299 (2021).
12. B. Surtees, S. Young, Y. Hu, G. Wang, E. McChesney, G. Kuroki, P. Acree, S. Thomas, T. Blair, S. Rastogi, D. L. Kraitchman, C. Weiss, S. Sukumar, S. C. Harvey, and N. J. Durr, "Validation of a low-cost, carbon dioxide-based cryoablation system for percutaneous tumor ablation," PLOS ONE 14(7), e0207107 (2019).
13. P. Ye, H. Yin, X. Gu, Y. Ye, Q. Zhao, Z. Chang, B. Han, X. Chen, and P. Liu, "Improved synergetic therapy efficiency of cryoablation and nanoparticles for MCF-7 breast cancer," Nanomedicine 13, 1889–1903 (2018).

14. R. C. Ward, A. P. Lourenco, and M. B. Mainiero, "Ultrasound-guided breast cancer cryoablation," American Journal of Roentgenology 213(3), 716–722 (2019).
15. T. G. Kotova, V. I. Kochenov, T. E. Potemina, and S. N. Tsybusov, "Circular cryogenic excision in surgical treatment of skin melanoma," Modern Technologies in Medicine 10(3), 52–56 (2018).
16. M. T. Chang, S. Song, and P. H. Hwang, "Cryosurgical ablation for treatment of rhinitis: A prospective multicenter study," The Laryngoscope 130(8), 1877–1884 (2019).
17. N. Tsunoda, T. Kawai, M. Obara, S. Suzuki, I. Miyamoto, Y. Takeda, and H. Yamada, "Analysis of effects and indications of cryosurgery for oral mucoceles," Journal of Stomatology, Oral and Maxillofacial Surgery 122(3), 267–272 (2021).
18. D. Theodorescu, "Cancer cryotherapy: evolution and biology," Reviews in Urology 6(Suppl. 4), S9–S19 (2004).
19. H. Nomori, I. Yamazaki, T. Kondo, and M. Kanno, "The cryoablation of lung tissue using liquid nitrogen in gel and in the ex vivo pig lung," Surgery Today 47, 259–264 (2017).
20. I. Burkov, A. Pushkarev, S. Ryabikin, A. V. Shakurov, D. I. Tsiganov, and A. A. Zherdev, "Numerical simulation of controlled precision cryosurgery using argon Joule–Thomson and liquid nitrogen evaporation cryoprobes," International Journal of Refrigeration 133, 30–40 (2022).
21. I. Burkov, A. Pushkarev, A. V. Shakurov, D. I. Tsiganov, and A. A. Zherdev, "Numerical simulation of multiprobe cryoablation synergy using heat source boundary," International Journal of Heat and Mass Transfer 147, 118946 (2020).
22. A. Shakurov, A. Pushkarev, V. Pushkarev, and D. I. Tsiganov, "Prerequisites for developing new generation cryosurgical devices," Modern Technologies in Medicine 9(2), 178–187 (2017).
23. A. Dhaliwal, S. Saghir, H. Mashiana, A. Braseth, B. S. Dhindsa, D. Ramai, P. Taunk, R. Gomez-Esquivel, A. Dam, J. Klapman, and D. G Adler, "Endoscopic cryotherapy: Indications, techniques, and outcomes involving the gastrointestinal tract," World Journal of Gastrointestinal Endoscopy 14(1), 17–28 (2022).
24. A. Pushkarev, "Heat transfer in cryosurgical device with an extended applicator," Journal of Physics: Conference Series 1683, 022049 (2020).
25. A. Bobrikhin, A. Gudkov, D. Tsyganov, S. V. Agasieva, E. N. Gorlacheva, V. Yu. Leushin, and V. D. Shashurin, "Compact self-contained cryosurgical devices," Biomedical Engineering 51, 120–123 (2017).
26. L. Dombrovsky, N. Nenarokomova, D. Tsiganov, and Y. A. Zeigarnik, "Modeling of repeating freezing of biological tissues and analysis of possible microwave monitoring of local regions of thawing," International Journal of Heat and Mass Transfer 89, 894–902 (2015).
27. M. L. Etheridge, J. Choi, S. Ramadhyani, and J. C. Bischof, "Methods for characterizing convective cryoprobe heat transfer in ultrasound gel phantoms," Journal of Biomechanical Engineering 135(2), 021002 (2013).
28. L. Massalha, A. Shitzer, "Freezing by a flat, circular surface cryoprobe of a tissue phantom with an embedded cylindrical heat source simulating a blood vessel," Journal of Biomechanical Engineering 126(6), 736–744 (2005).
29. J. Goette, T. Weimar, M. Vosseler, M. Raab, U. Walle, M. Czesla, and N. Doll, "Freezing equals freezing? Performance of two cryoablation devices in concomitant mitral valve repair," Thoracic and Cardiovascular Surgeon 64(08), 672–678 (2016).
30. G. Katyba, K. Zaytsev, I. Dolganova, I. A. Shikunova, N. V. Chernomyrdin, S. O. Yurchenko, G. A. Komandin, I. V. Reshetov, V. V. Nesvizhevsky, and V. N. Kurlov, "Sapphire shaped crystals for waveguiding, sensing and exposure applications," Progress in Crystal Growth and Characterization of Materials 64(4), 133–151 (2018).
31. V. Kurlov, "Sapphire: Properties, growth, and applications," in Encyclopedia of Materials: Science and Technology, K. J. Buschow, R. W. Cahn, M. C. Flemings, B. Ilschner, E. J. Kramer, S. Mahajan, and P. Veyssière (Eds.), Elsevier, Oxford, 8259–8264 (2001).
32. H. LaBelle, A. Mlavsky, "Growth of controlled profile crystals from the melt: Part I – sapphire filaments," Materials Research Bulletin 6(7), 571–579 (1971).
33. H. LaBelle, "Growth of controlled profile crystals from the melt: Part II – Edge-defined, Film-fed Growth (EFG)," Materials Research Bulletin 6(7), 581–589 (1971).
34. B. Chalmers, H. LaBelle, and A. Mlavsky, "Growth of controlled profile crystals from the melt: Part III – theory," Materials Research Bulletin 6(8), 681–690 (1971).
35. V. Kurlov, "The noncapillary shaping (NCS) method: a new method of crystal growth," Journal of Crystal Growth 179(1–2), 168–174 (1997).
36. V. N. Kurlov, S. N. Rossolenko, "Growth of shaped sapphire crystals using automated weight control," Journal of Crystal Growth 173(3–4), 417–426 (1997).
37. I. Agafonkina, A. Belozerov, Y. Berezovsky, I. A. Korolev, A. V. Pushkarev, D. I. Tsiganov, A. V. Shakurov, and A. A. Zherdev, "Thermal properties of biological tissue gel-phantoms in a wide low-temperature range," Journal of Engineering Physics and Thermophysics 94, 790–803 (2021).
38. I. Agafonkina, A. Belozerov, A. Vasilyev, A. V. Pushkarev, D. I. Tsiganov, A. V. Shakurov, and A. A. Zherdev, "Thermal properties of human soft tissue and its equivalents in a wide low-temperature range," Journal of Engineering Physics and Thermophysics 94, 233–246 (2021).

39. V. N. Kurlov, B. M. Epelbaum, "Fabrication of near-net-shaped sapphire domes by noncapillary shaping method," Journal of Crystal Growth 179, 175–180 (1997).
40. H. LaBelle, "EFG, the invention and application to sapphire growth," Journal of Crystal Growth 50(1), 8–17 (1980).
41. V. N. Kurlov, S. N. Rossolenko, N. V. Abrosimov, and K. Lebbou, "Shaped Crystal Growth," Chapter 5 in Crystal Growth Processes Based on Capillarity: Czochralski, Floating Zone, Shaping and Crucible Techniques, T. Duffar (Ed.), John Wiley & Sons, Chichester, UK, 277–354 (2010).
42. P. I. Antonov, V. N. Kurlov, "A review of developments in shaped crystal growth of sapphire by the Stepanov and related techniques," Progress in Crystal Growth and Characterization of Materials 44(2), 63–122 (2002).
43. N. Abrosimov, V. Kurlov, and S. Rossolenko, "Automated control of Czochralski and shaped crystal growth processes using weighing techniques," Progress in Crystal Growth and Characterization of Materials 46(1–2), 1–57 (2003).
44. J. W. Ekin, Experimental Techniques for Low-Temperature Measurements: Cryostat Design, Material Properties and Superconductor Critical-Current Testing, Oxford University Press, New York (2006).
45. N. R. Mitra, D. L. Decker, and H. B. Vanfleet, "Melting curves of copper, silver, gold, and platinum to 70 kbar," Physical Review 161(3), 613–617 (1967).
46. B. Rubinsky, "Cryosurgery," Annual Review of Biomedical Engineering 2, 157–187 (2000).
47. F. Dumont, P.-A. Marechal, and P. Gervais, "Involvement of two specific causes of cell mortality in freeze-thaw cycles with freezing to –196 °C," Applied and Environmental Microbiology 72(2), 1330–1335 (2006).
48. A. A. Gage, J. Baust, "Mechanisms of tissue injury in cryosurgery," Cryobiology 37(3), 171–186 (1998).
49. P. Mazur, "Freezing of living cells: mechanisms and implications," American Journal of Physiology – Cell Physiology 247, C125–C142 (1984).